Inventory of Supplemental Information

While all the supplementary data is essential control data (as outlined below), space constraints preclude their incorporation into the main figures.

Supplemental Figure S1

This figure is a repeat of the data presented in Figure 1A-F, but using FAb fragments of the SUK4 and 9E10 antibodies rather than whole antibodies. These results further support the key findings in Figure 1A-F and are an additional control further demonstrating that the affect on mIPSC amplitudes mediated by the SUK4 whole antibody is mediated by the antigen binding region of the antibody (the FAb fragment).

Supplemental Figure S2

This figure is an additional control for the data presented in Figure 1G-H, demonstrating antibody penetrance in treated neuronal cultures. These results are therefore an important additional control demonstrating validity of the experimental approach to transduce neurons with the function blocking antibody.

Supplemental Figure S3

This figure is additional data for experiments included in Figures 1G-H, 4F-G, 6F-G and 7I-J (Panels A, B, C and D respectively in Supplemental Figure S3). These results demonstrate that treatments and molecular interventions do not alter the synaptic to non-synaptic ratio of $GABA_AR$ clusters and so further supports the body of data outlining changes in the number of post-synaptic $GABA_ARs$.

Supplemental Figure S4

Panels A and B are the whole neurons used in Figure 2 A and B respectively, demonstrating the localisation of the KIF5 and $GABA_AR$ $\gamma 2$ subunits in neurons. Panels C and D are additional controls produced in response to reviewers comments and demonstrate that the reported co-localisation observed in Figure 2A&B is not due chance alone.

Supplemental Figure S5

This figure shows additional data regarding the HAP1-KIF5 interaction and mapping of the interaction domains. Panels A and B demonstrates the HAP1-KIF5 interaction by an additional experimental procedure, (immuno-precipitation from transfected cells). C and D show the binding of full length HAP1 to the shortest KIF5 fragment, data not shown in main figure, but a control to indicate that the KIF5-HBD would bind to full length endogenous HAP1 in cells. As such these data support that in Figure 3.

Supplemental Figure S6

Additional control data requested by reviewers, firstly demonstrating that surface populations of other receptors are not affected by the expression of

KIF5B-HBD and secondly showing that endocyctosis of $GABA_A$Rs is similarly unaffected. These results support the specificity of the effects reported in Figure 3D-H.

Supplemental Figure S7

This figure demonstrates that the effect on mIPSC amplitudes mediated by and KIF5C-HBD is similar to that mediated by KIF5B-HBD which is agreement with the in vitro binding experiments in Figure 2O-P and which further supports the role of KIF5 motors in regulating $GABA_A$R trafficking.

Supplemental Figure S8

This is an additional control demonstrating that the affect on $GABA_A$R mIPSCs is specific to the KIF5 motors and not other KIF motors (e.g. KIF17) and further supports the specificity of KIF5 motors for $GABA_A$R transport.

Supplemental Figure S9

Additional control data requested by reviewers firstly demonstrating that surface populations of other receptors are not affected by knockdown of HAP1 expression and secondly showing that endocytosis of $GABA_A$Rs is similarly unaffected.

Supplemental Figure S10

This figure illustrates the new RNAi vector designed to co-express a reporter for $GABA_A$R trafficking (A and B) and confirms the shRNAi is still functional in the new vector (expressing γ2-GFP instead of GFP; C and D). These results confirm the efficiency of the new RNAi vector and are therefore an important control.

Supplemental Figure S11

Supporting additional control data requested by the reviewers, which illustrates that there is no additional affect of the KIF5B-HBD when expressed on a mutant polyQ-htt background, suggesting that the two mutants act in the same pathway. Thus, these experiments extend the results shown in Figure 7A-C.

Supplemental Table S1

Kinetic analysis of mIPSC recordings requested by the reviewers which demonstrates that there was no change in the kinetics of the mIPSCs.

Supplemental Movies S1 and S2

These are representative movies of data analysed used for the experiment in Figure 7. For this particular experiment a movie was the best way to demonstrate vesicular movements.

Supplemental Materials Table of Contents

Supplemental Movie Legends

Movie S1. +/+ cell transfected with α1, β3 and $\gamma2^{GFP}$ to form GFP tagged $GABA_AR$ labelled vesicles.

Movie S2. 109Q/109Q cell transfected with α1, β3 and $\gamma2^{GFP}$ to form GFP tagged $GABA_AR$ labelled vesicles.

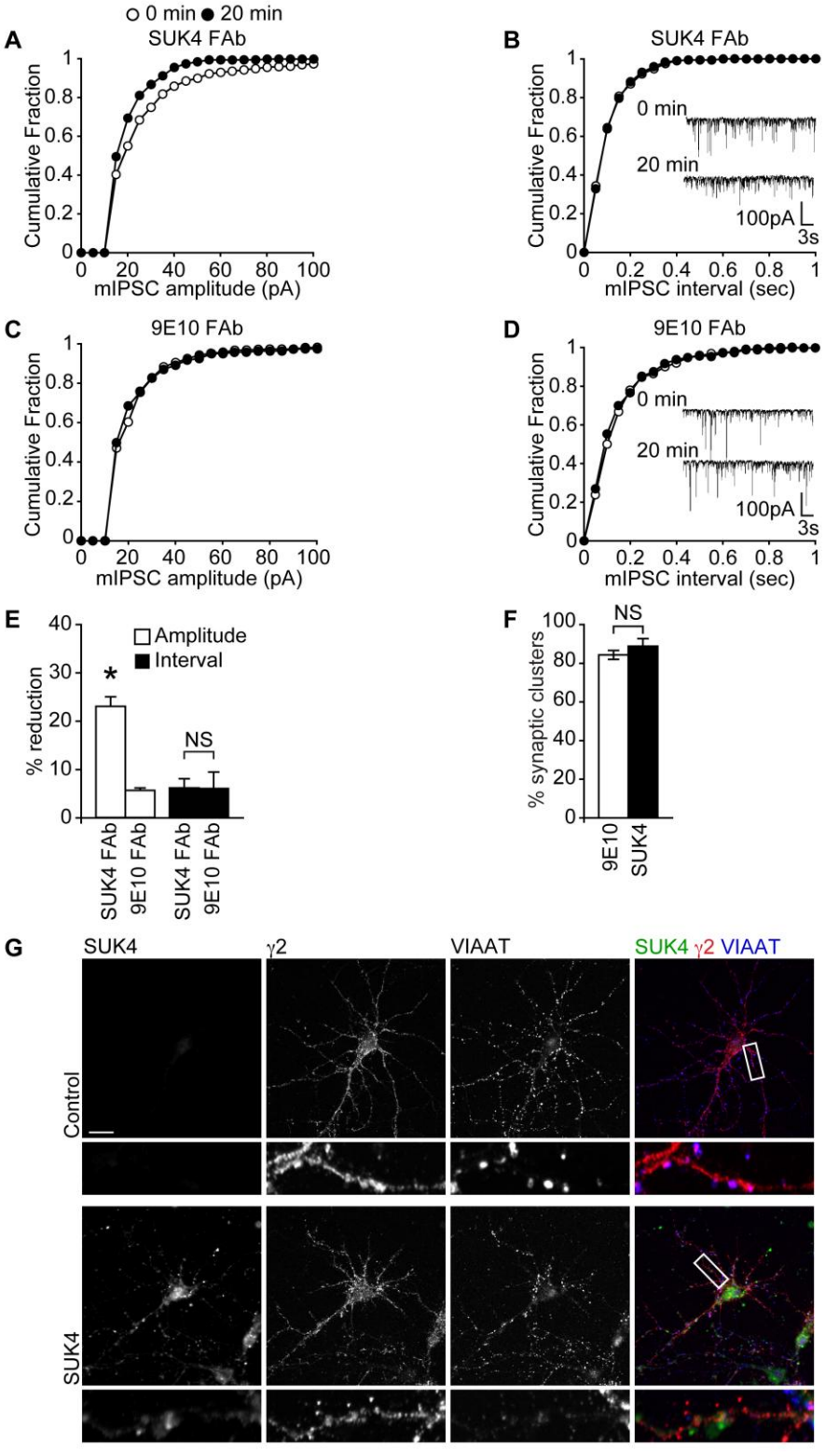

Supplemental Figure S1

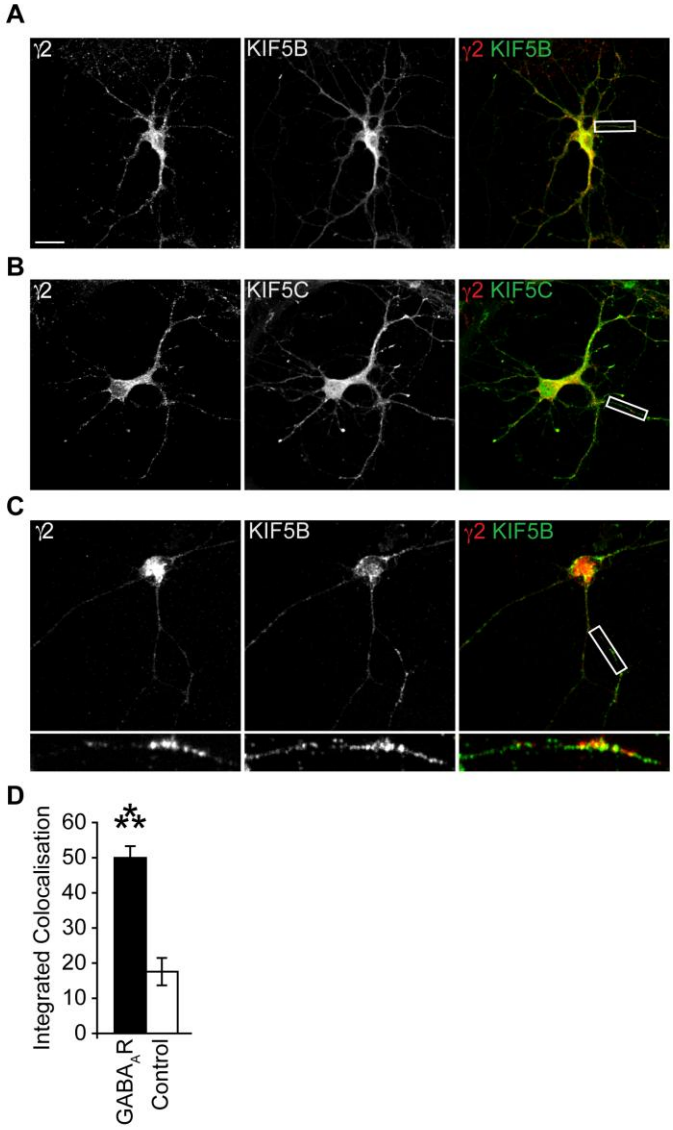

Supplemental Figure S2

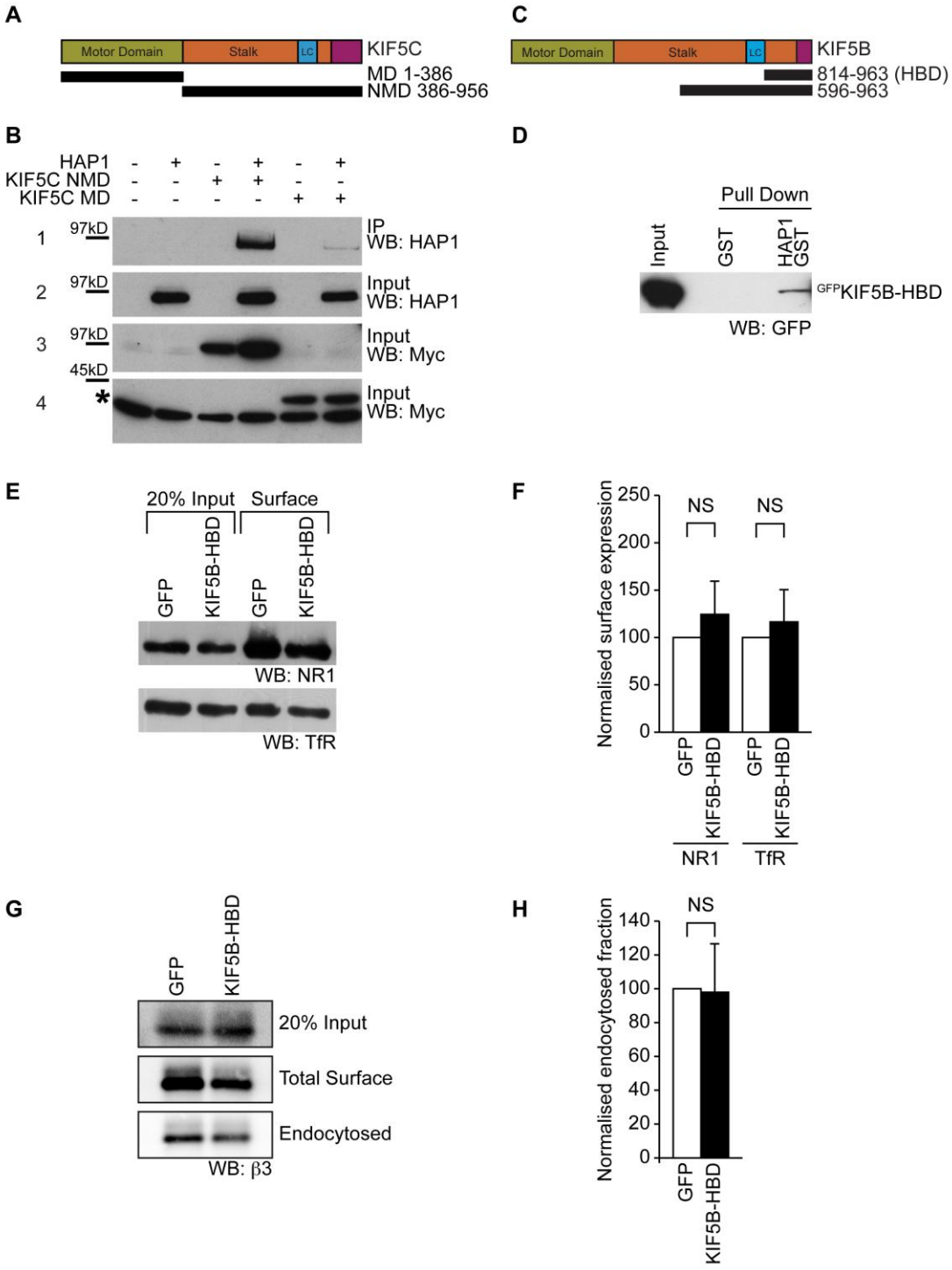

Supplemental Figure S3

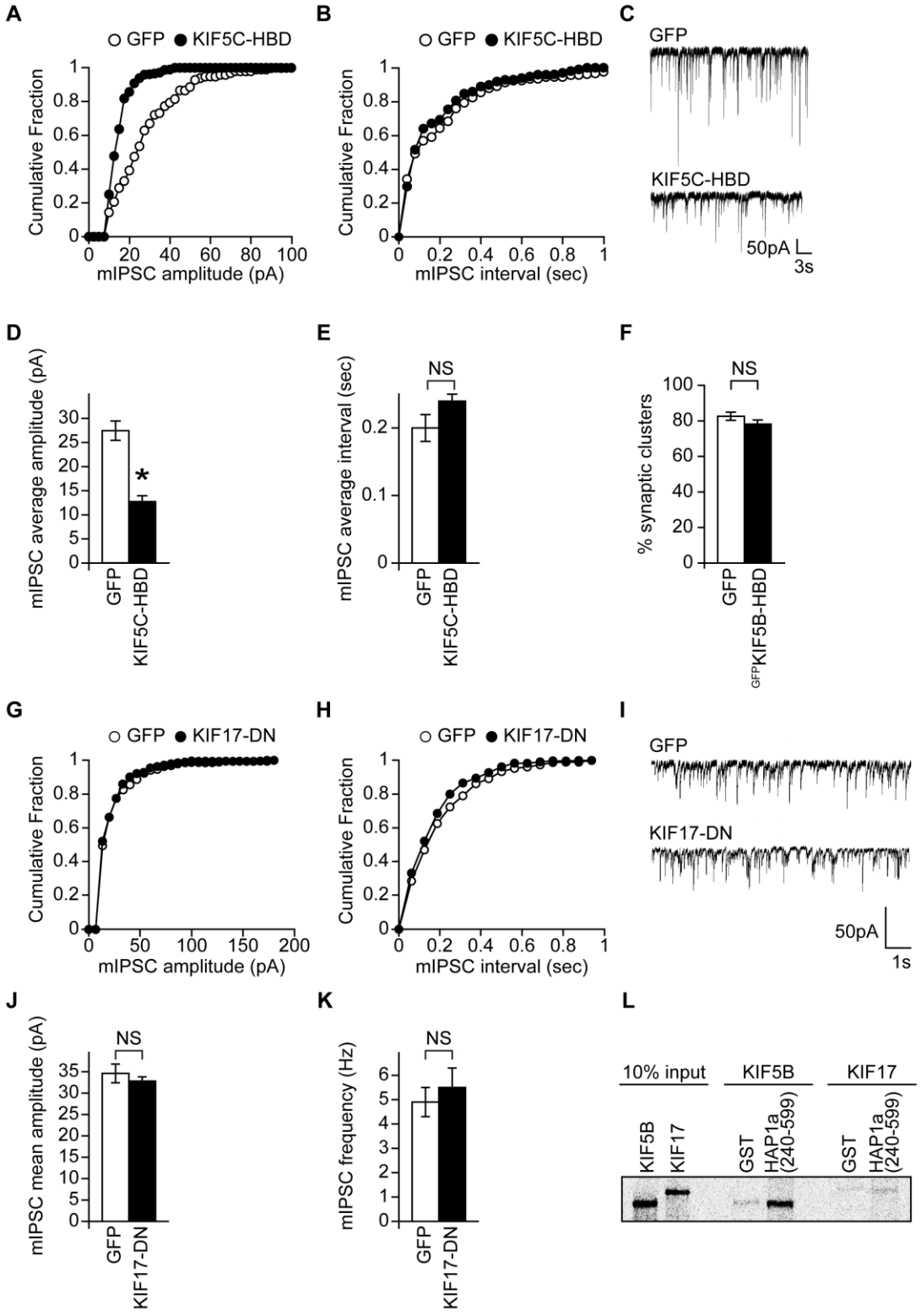

Supplemental Figure S4

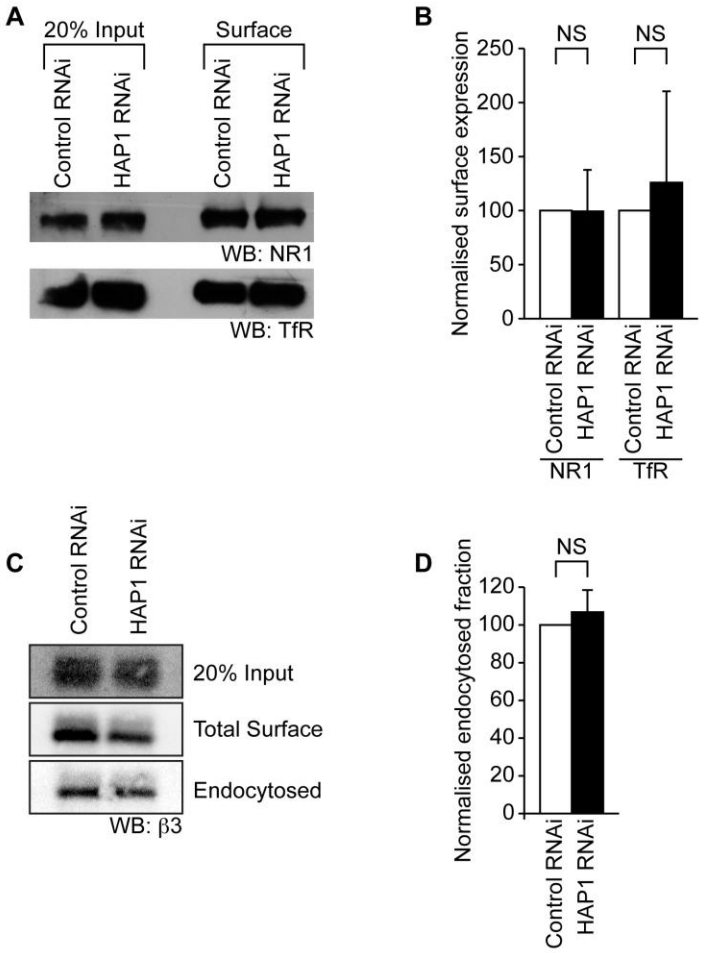

Supplemental Figure S5

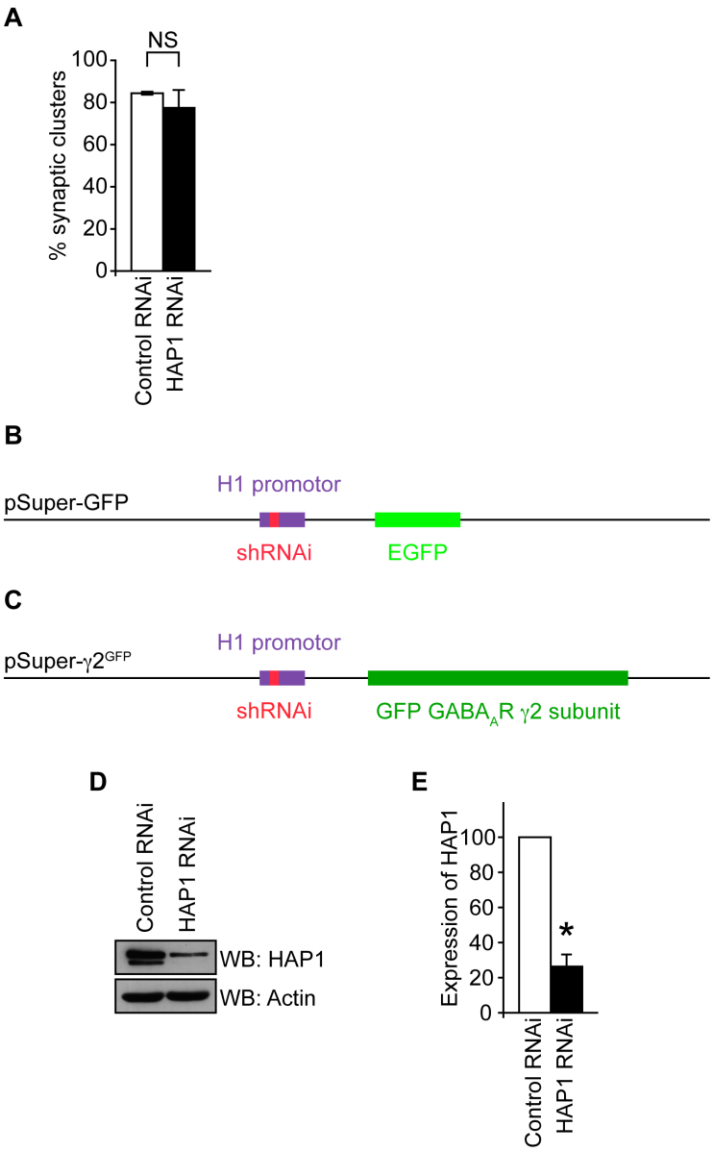

Supplemental Figure S6

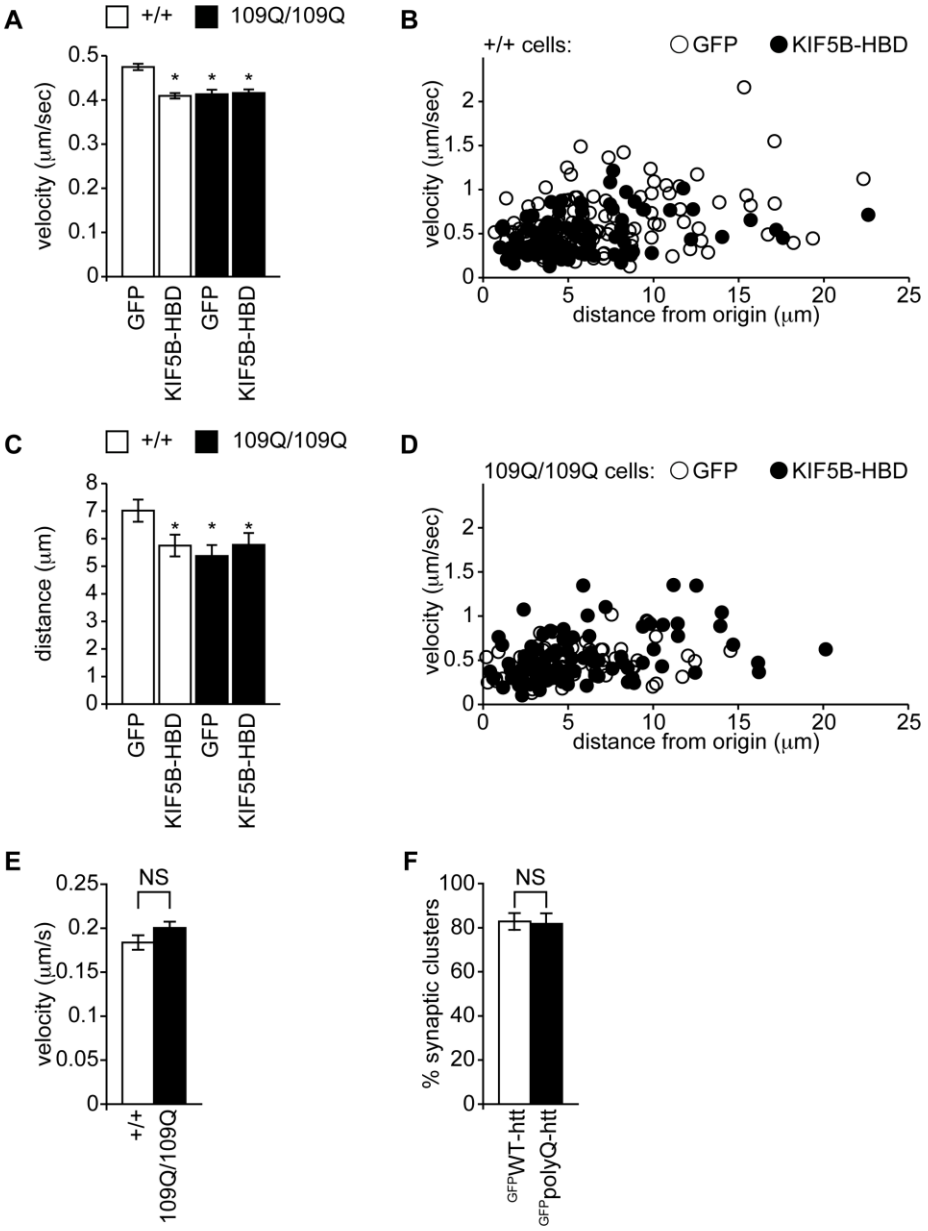

Supplemental Figure S7

Supplemental Figure Legends

Supplemental Figure S1.

(A-E) Whole-cell recordings of mIPSCs in neurons dialyzed with either SUK4 or control 9E10 FAb fragment antibodies. Cumulative distribution plots (A-D) showed that the mIPSC amplitude shifted leftward in SUK4 FAb-dialyzed neurons at t = 20 compared to t = 0 min (A), whilst there was no change in mIPSC interval (B). No effect was observed on either mIPSC amplitude (C) or interval (D) in neurons dialyzed with the control 9E10 FAb antibodies. (Inset, A and C) Representative traces demonstrating reduction in mIPSC sizes upon dialysis of SUK4, but not control 9E10 FAb antibody. Summary bar graph (E) shows the percentage (mean ± s.e.m.) reduction of mIPSC amplitude and interval produced by 9E10 or SUK4 after 20 minutes of FAb antibody dialysis (Amplitude: SUK4, 23.0±2% reduction in amplitude, n = 6; 9E10, 5.6±0.5% reduction, n = 5; *, $P < 0.05$. Interval: SUK4, 6.1±1.9% reduction in interval; 9E10 6.0±3.4% reduction.).

(F) The surface immunolabelled γ2 subunit clusters of SUK4 or control treated neurons were scored for being synaptic or extrasynaptic by their apposition to the inhibitory pre-synaptic marker Vesicular Inhibitory Amino Acid Transporter (VIAAT). There was no significant change in the percentage of $GABA_AR$ γ2 subunit clusters associated with pre-synaptic terminals. Error bars, s.e.m. 9E10 treated neurons 84.3±2.3% synaptic, SUK4 treated neurons 88.8±3.9% synaptic, n = 5, $P = 0.35$ (Student's *t*-test).

(G) Chariot reagent transduces the function blocking KIF5 antibody SUK4 into neurons. Neurons were treated with complexes of Chariot reagent and the SUK4 antibody, or mock treated with Chariot reagent alone, for 24 hours before fixation and surface immunostaining with guinea pig anti-$GABA_AR$ γ2 antibody, followed by permeabilisation and immunostaining with rabbit anti-VIAAT. The secondary antibody AlexaFluor 488 conjugated goat anti-mouse was used to detect cells transduced with SUK4. Scale bar = 10μm, boxed dendrites = 25μm.

Supplemental Figure S2.

(A-D) Endogenous localisation of KIF5 in neurons**.** (A and B) Hippocampal neurons co-stained with antibodies to the $GABA_AR$ γ2 subunit (A and B; red) and either anti-KIF5B (A) or anti-KIF5C (B) (green), scale bar = 10 μm. Regions of colocalization for both KIF5B and KIF5C could be detected (yellow). Boxed dendrites in A and B are those in Figure 2A and B, respectively. (C) Cortical neuron co-stained with antibodies to the $GABA_AR$ γ2 subunit (red) and KIF5B (green). Straightened 25μm sections of dendrite (boxed) were analysed for the integrated colocalisation of $GABA_ARs$ with KIF5B and compared to the integrated colocalisation of the control ($GABA_AR$ plane rotated 180º) with KIF5B. (D) Summary bar graph, integrated colocalisation of $GABA_ARs$ with KIF5B is 50.2±3.3% compared to 17.3±3.9% for the control. Error bars, s.e.m.; n = 13; $P < 0.0001$ (Student's *t*-test).

Supplemental Figure S3.

(A-D) Co-expression of KIF5 fragments and HAP1. (A) Schematic map of Motor Domain (MD) and Non-Motor Domain (NMD) constructs. (B) Immunoprecipitation from transfected HEK cells. Anti-9E10 is only able to immunoprecipitate ^{HA}HAP1 when HEK cells are co-transfected with ^{9E10}KIF5C-NMD, but not ^{9E10}KIF5C-MD (B, panel 1). Expression of HAP1 (B**,** panel 2), ^{9E10}KIF5C-NMD (B**,** panel 3), and ^{9E10}KIF5C-MD (B**,** panel 4) were confirmed by western blotting input samples of the same transfected cell lysates (* denotes a cross reacting band detected by 9E10 antibody in all lanes). (C) Schematic map of ^{GFP}KIF5B (596-963) and ^{GFP}KIF5B (814-963) constructs. (D) ^{GFP}KIF5B (814-963) is sufficient for binding to HAP1 and called the ^{GFP}KIF5B-**H**AP1 **B**inding **D**omain (HBD). ^{GFP}KIF5B-HBD is pulled down by a HAP1-GST fusion protein from transfected COS cells.

(E-F) Expression of KIF5B-HBD does not have a significant effect on the surface expression of either NMDA receptor NR1 subunits or transferrin receptors (TfR) in neurons as revealed by surface biotinylation and western blotting with specific antibodies (E). (F) Surface levels

of receptors were expressed as a fraction of the total number of receptors before percentage surface expression was normalised to GFP. NR1 surface expression in KIF5B-HBD expressing neurons was 124.4±35.0%, n = 6, no significant difference. TfR surface expression in KIF5B-HBD expressing neurons was 116.4±34.0%, n = 6, no significant difference.

(G-H) Endocytosis of $GABA_A$Rs does not change in neurons transfected with KIF5B-HBD. Surface labeled receptors were allowed to endocytose for 30 minutes before the remaining surface label was cleaved leaving a protected pool of endocytosed receptors, which were purified and detected by western blotting (G). (H) Summary bar graph of endocytosed receptors, expressed as a fraction of the total surface population and normalised as a percentage of the control GFP. Endocytosed population $GABA_A$Rs was 98.0±28.7% of GFP control in KIF5B-HBD transfected neurons, n = 3, not significant.

Supplemental Figure S4.

(A-E) Whole-cell recordings of mIPSCs from neurons transfected with KIF5C-HBD or GFP control. Cumulative distribution plots (A and B) show the mIPSC amplitude shifts to smaller amplitudes in neurons transfected with KIF5C-HBD (A), whilst there is no change in mIPSC interval (B). (C) Representative traces demonstrating reduction in mIPSC sizes in cells transfected with KIF5C-HBD, compared to GFP-transfected cells. Summary bar graphs (D and E) show the average (mean ± s.e.m.) mIPSC amplitude and interval of transfected neurons (KIF5C-HBD, n = 8; GFP, n = 6; *, $P < 0.05$).

(F) The surface immunolabelled γ2 subunit clusters of ^{GFP}KIF5B-HBD or control transfected neurons were scored for being synaptic or extrasynaptic by their apposition to the inhibitory pre-synaptic marker Vesicular Inhibitory Amino Acid Transporter (VIAAT). There was no change in the percentage of $GABA_A$R γ2 subunit clusters associated with pre-synaptic terminals. Error bars, s.e.m. GFP transfected neurons 82.6±2.3% synaptic, ^{GFP}KIF5B-HBD 78.2±4.3% synaptic, n = 5, $P = 0.4$ (Student's *t*-test).

(G-K) Whole cell recordings of mIPSCs neurons transfected with KIF17-DN or GFP control. Cumulative distribution plots (G and H) show no change in mIPSC amplitude or interval in neurons transfected with KIF17-DN (KIF17 Dominant Negative). (I) Representative traces demonstrating no affect on mIPSC in cells transfected with KIF17-DN, compared to GFP-transfected cells. Summary bar graphs (J and K) show the average (mean ± s.e.m.) mIPSC amplitude (GFP: 34.6±2.2 pA; KIF17-DN: 32.8±1.0 pA) and frequency (GFP: 4.9±0.6 Hz; KIF17-DN: 5.5±0.8 Hz) of transfected neurons (KIF17-DN, n = 8; GFP n = 11; no significant differences).

(L) *In vitro* translated and ^{35}S radiolabelled KIF5B or KIF17 were subjected to pull down by HAP1(240-599)-GST and bound protein separated by SDS-PAGE and detected by phosphor storage screen. HAP1(240-599) interacted with KIF5B, but not KIF17.

Supplemental Figure S5.

(A-B) Expression of HAP1 RNAi does not have a significant effect on the surface expression of either NMDA receptor NR1 subunits or transferrin receptors (TfR) in neurons as revealed by surface biotinylation and western blotting with specific antibodies (A). (B) Surface levels of receptors were expressed as a fraction of the total number of receptors before percentage surface expression was normalised to control RNAi. NR1 surface expression in HAP1 RNAi expressing neurons was 99.3±38.4%, n = 4, no significant difference. TfR surface expression in KIF5B-HBD expressing neurons was 125.9±84.4%, n = 3, no significant difference.

(C-D) Endocytosis of $GABA_A$Rs does not change in neurons transfected with HAP1 RNAi. Surface labelled receptors were allowed to endocytose for 30 minutes before the remaining surface label was cleaved leaving a protected pool of endocytosed receptors, which were purified and detected by western blotting (C). (D) Summary bar graph of endocytosed receptors, expressed as a fraction of the total surface population and normalised as a percentage of the control RNAi. Endocytosed population $GABA_A$Rs was 106.8±11.7% of control RNAi in HAP1 RNAi transfected neurons, n = 3, not significant.

Supplemental Figure S6.

(A) The surface immunolabelled γ2 subunit clusters of HAP1 RNAi or control transfected neurons were scored for being synaptic or extrasynaptic by their apposition to the inhibitory pre-synaptic marker Vesicular Inhibitory Amino Acid Transporter (VIAAT). There was no change in the percentage of $GABA_AR$ γ2 subunit clusters associated with pre-synaptic terminals. Error bars, s.e.m. Scrambled RNAi control transfected neurons 84.4±0.7% synaptic, HAP1 RNAi 77.5±8.4% synaptic, n = 3, $P = 0.45$ (Student's *t*-test).

(B-E) pSuper-$\gamma2^{GFP}$ vector. (B) Schematic diagram of the original pSuper vector containing the shRNAi sequence, H1 promoter and GFP expression marker. (C) Schematic diagram of the new pSuper vector expressing $\gamma2^{GFP}$ in place of GFP. (D-E) pSuper-$\gamma2^{GFP}$ HAP1 RNAi was checked for ability to knock-down the expression of HAP1 in transfected neurons. (D) Western blots of transfected neuronal lysates showing decreased expression of HAP1 with the pSuper-$\gamma2^{GFP}$ HAP1 RNAi compared to pSuper-$\gamma2^{GFP}$ Control RNAi. (E) Summary bar graph of knock down. HAP1 expression is 26.3±6.8% of control in neurons expressing HAP1 RNAi. Error bars, s.e.m.; n = 3; $P < 0.01$.

Supplemental Figure S7.

(A-D) The affect of KIF5B-HBD on $GABA_AR$ trafficking in wild type or mutant huntingtin cells. WT (+/+) or 109Q/109Q neuronal cells expressing α1, β3 and $^{DsRed}\gamma2$ subunits and either KIF5B-HBD or GFP control were used to analyse the trafficking of $^{DsRed}GABA_AR$ vesicles in real time by video microscopy. (A) Average velocity ± s.e.m (μm/sec) of moving vesicles was reduced in 109Q/109Q cells also expressing GFP and +/+ also expressing KIF5B-HBD compared to +/+ control cells also expressing GFP. 109Q/109Q cells also expressing KIF5B-HBD showed no additional effect on the velocity of $GABA_AR$ vesicles by KIF5B-HBD compared to 109Q/109Q cells also expressing GFP. Velocity in +/+ GFP cells, 0.47±0.007μm/s, n = 7207 measures (14 cells); +/+ KIF5B-HBD cells, 0.41±0.006μm/s, n = 8647 measures (14 cells); 109Q/109Q GFP cells, 0.41±0.01μm/s, n = 3340 measures (10

cells); 109Q/109Q KIF5B-HBD cells, 0.42±0.008μm/s, n = 5274 measures, (12 cells). (B) The distance from origin vs. the average velocity of each vesicle track was plotted for the +/+ cells. The main population of $^{DsRed}GABA_AR$ vesicles in +/+ cells expressing KIF5B-HBD move more slowly and for shorter distances compared to control GFP cells. (C) Similar to results in (A), the mean distance ± s.e.m (μm) each vesicle has moved from its origin is longer in +/+ cells transfected with GFP compared to all other transfected cell types demonstrating a decreased processivity in mutant 109Q cells and +/+ cells expressing KIF5B-HBD. Distance from origin in +/+ GFP cells, 7.02±0.40μm, n = 115 measures (14 cells); +/+ KIF5B-HBD cells, 5.75±0.39μm, n = 95 measures (14 cells); 109Q/109Q GFP cells, 5.37±0.40μm, n = 65 measures (10 cells); 109Q/109Q KIF5B-HBD cells, 5.78±0.43μm, n = 87 measures, (12 cells). (D) The distance from origin vs. the average velocity of each vesicle track was plotted for the 109Q/109Q cells. Populations of $^{DsRed}GABA_AR$ vesicles in 109Q/109Q cells expressing KIF5B-HBD or GFP move at similar velocities for similar distances.

(E) Mitochondrial motility in +/+ cells or 109Q/109Q +/+ cells or 109Q/109Q cells were transfected with mtDsRed, a mitochondrially targeted DsRed protein. The velocity of mitochondria was unchanged in the mutant huntingtin expressing cells. Velocity in +/+ cells, 0.18±0.008μm/s, n = 1767 measures; velocity in 109Q/109Q cells, 0.20±0.007μm/s, n = 2222 measures; 13 cells each over 3 independent experiments.

(F) The surface immunolabelled γ2 subunit clusters of ^{GFP}WT-htt or ^{GFP}polyQ-htt transfected neurons were scored for being synaptic or extrasynaptic by their apposition to the inhibitory pre-synaptic marker Vesicular Inhibitory Amino Acid Transporter (VIAAT). There was no change in the percentage of $GABA_AR$ γ2 subunit clusters associated with pre-synaptic terminals. Error bars, s.e.m. ^{GFP}WT-htt transfected neurons 82.8±3.8% synaptic, ^{GFP}polyQ-htt 81.7±4.8% synaptic, n = 5, $P = 0.85$ (Student's *t*-test).

	Rise time (10-90%) (ms)	n	Tau (ms)	n
GFP	3.0 ± 0.6	7	7.9 ± 0.4	7
KIF5B-HBD	3.3 ± 0.7	7	7.5 ± 0.9	7
SUK4 before	2.9 ± 0.8	6	7.8 ± 0.7	6
SUK4 after	2.7 ± 0.5	7	8.3 ± 0.8	7

Supplemental Table S1. Kinetic analysis of mIPSC recordings.

Supplemental Experimental Procedures

Antibodies

The following primary antibodies were used: monoclonal anti-HAP1 antibody recognizing HAP1a and HAP1b (BD Transduction laboratories) (WB 1:250), goat anti-HAP1 N-terminal antibody recognising HAP1a and HAP1b (Santacruz) (IP 1-2μg), rabbit anti-KIF5B (Abcam) (WB 1:500, IF 1:100), rabbit anti-KIF5C (Abcam) (WB 1:500, IF 1:100), mouse anti-Kinesin Heavy Chain [H2] (Abcam) (WB 1:500), rabbit anti-Myc (Santacruz) (IF 1:100, IP 1μg), mouse anti-GFP (Roche) (WB 1:500), rabbit anti-VIAAT (a kind gift from B. Gasnier, (Dumoulin et al., 1999) (IF 1:1000), mouse anti-NMDAR1 54.1 (BD Transduction laboratories) (WB 1:500), mouse anti-Human Transferrin Receptor H68.4 (Invitrogen) (WB 1:100), guinea pig anti-γ2 (serum, (Kittler et al., 2001)) (IF 1:100). Rabbit anti-β3 was raised against MBP-β3-(345-408) and purified on a GST-β3-(345-408) column. The SUK4 hybridoma recognising KIF5A-C was obtained from the Developmental Studies Hybridoma Bank. The monoclonal antibodies anti-KIF5 and anti-myc were obtained from SUK4 and 9E10 hybridoma cells respectively, grown in Integra CL350 concentrating flasks and supernatant used directly for western blotting and immunofluorescence. SUK4 and 9E10 antibodies used for Chariot treatments were purified by using Protein G sepharose beads (Generon).

Plasmid Constructs

Full-length rat HAP1a C-terminally tagged with HA in a pRK5 expression vector (pRK5-HAP1a-HA) and GST HAP1 have been previously described (Kittler et al., 2004; Li et al., 1995). α1, β3, γ2-GFP cDNAs used for striatal cell-line transfection have been described previously (Kittler et al., 2005), as have pEGFP-htt-17Q (WT htt) and pEGFP-htt-68Q (polyQ htt) (Gauthier et al., 2004). γ2-DsRed was created by replacing the GFP tag using XhoI sites with monomeric DsRed created by PCR.

Full-length mouse kinesin heavy chains, KIF5A, KIF5B, and KIF5C were N-terminally c-Myc tagged in a pRK5 expression vector giving the constructs pRK5-Myc-KIF5A, pRK5-

Myc-KIF5B, pRK5-Myc-KIF5C. The kinesin light chain used was KLC-1, highly expressed in neurons (Rahman et al., 1998), and similarly N-terminally c-Myc tagged to give pRK5-Myc-KLC1. Two KIF5B fragments corresponding to the C-terminal 367 and 149 residues were cloned by PCR from the full-length construct. The resulting fragments were given an N-terminal EGFP tag in the pEGFP-C1 vector using the restriction enzymes EcoRI and BamHI to create pEGFP-C1-KIF5B-(596-963) and pEGFP-C1-KIF5B-(814-963). The deletion constructs of KIF5C used in the supplementary data were from Anne Stephenson. KIF5C was split into its motor domain (MD, residues 1-335) and non-motor domain, (NMD, residues 336-957), each being cloned into the modified mammalian expression vector, pCMVTag4a, to generate the N-terminally c-Myc tagged constructs pCMV-KIF5C-(1-335) and pCMV-KIF5C-(336-957) (Smith et al., 2006).

Each of the HAP1a truncations were cloned into pGEX-4T-GST by PCR. Constructs were cloned with the enzymes BamHI and EcoRI to create the following constructs: pGEX-4T-GST-HAP1a (153-599); pGEX-4T-GST-HAP1a (215-599); pGEX-4T-GST-HAP1a (240-599); pGEX-4T-GST-HAP1a (329-599); pGEX-4T-GST-HAP1a (371-599). GST vectors were expressed in E.coli BL21 for production and purification of GST fusion proteins as described previously by immobilization on glutathione agarose beads.

HAP1a (153-320)-GFP was created by digesting pRK5-Myc-HAP1a (153-320) with BamHI and EcoRI and ligating the resulting insert into pEGFP-C1 digested with BglII and EcoRI.

The RNAi target sequence for HAP1 (AAGCTACCGATCATCAACC) was designed by Oligoengine and cloned into pSuper.gfp+neo (Oligoengine) following the manufacturer's instructions. The scrambled control RNAi had the target sequence GGAATCTTCCTGCTTTGGG and was similarly cloned into pSuper.gfp+neo. For coexpression of RNAi sequences and $\gamma 2^{GFP}$ from the same vector, the neomycin-GFP reporter of pSuper.gfp+neo was replaced with $\gamma 2^{GFP}$ created by PCR using the enzymes NheI and NotI.

Immunofluorescence staining and cluster analysis

Coverslips containing neurons for surface staining or whole cell staining were fixed with 4% paraformaldehyde/4% sucrose/PBS pH7 solution for 4 or 10 minutes respectively. Coverslips were washed three times with PBS then blocked by incubation in block solution (PBS with 10% horse serum, 0.5% BSA) for ten minutes. Coverslips for whole cell staining were incubated in block solution also containing 0.2% Triton X-100. Primary and secondary antibodies were diluted in block solution and incubated with the coverslips for 1 hour at room temperature, with six brief washes of PBS between incubations. Coverslips were mounted onto a low iron, clear glass slides using ProLong Gold antifade reagent (Invitrogen) and sealed around the edge with nail varnish. In the case of neurons used for analysis of $GABA_AR$ synapses, coverslips were fixed and blocked for surface labelling with antibody serum against γ2-subunits overnight at 4°C. The following day coverslips were washed six times then permeabilised for ten minutes to allow subsequent penetration of inhibitory pre-synaptic marker rabbit anti-VIAAT and secondary antibodies Cy5 conjugated anti-rabbit and Alexa 594 conjugated anti-guinea pig. Chariot treated neurons were also stained with Alexa 488 conjugated anti-mouse (Molecular Probes). All images within a data set were obtained under the same conditions from the confocal microscope. Using Metamorph software, a suitable threshold was selected in a blind fashion for each data set and applied to all images. γ2 clusters above this threshold were measured and simultaneously scored for synaptic localization by proximity to the pre-synaptic marker VIAAT. Cultured hippocampal and striatal neurons were analyzed by immunofluorescence and Confocal Laser Scanning Microscopy (CLSM). Cells were viewed using a Zeiss LSM 510 META confocal microscope. All images were digitally captured with LSM software with excitation at 488nm for GFP, FITC and Alexa-Fluor 488, 568nm for Alexa-Fluor 543 and 633nm for Cy5 conjugated secondary antibodies. Pinholes were set to 1 Airy unit creating an optical slice of 0.8μm. Captured confocal images were analyzed using Metamorph software (Universal Imaging Corporation).

For quantification of the immunofluorescence colocalisation between $GABA_A$Rs and KIF5B cultured cortical neurons were labeled with antibodies to $GABA_A$Rs and to KIF5B and were imaged using confocal microscopy. 25μm sections of dendrite were straightened using the ImageJ plugin Straighten (Eva Kocsis), to allow us to then rotate the image plane of the dendrite by 180 degrees (see below). Integrated colocalisation of $GABA_A$Rs with KIF5B was assessed in Metamorph using a user-defined threshold and then the $GABA_A$R image plane was rotated 180 degrees to give a random distribution of $GABA_A$R and the integrated colocalisation was assessed again using the same thresholds.

Dumoulin, A., Rostaing, P., Bedet, C., Levi, S., Isambert, M.F., Henry, J.P., Triller, A., and Gasnier, B. (1999). Presence of the vesicular inhibitory amino acid transporter in GABAergic and glycinergic synaptic terminal boutons. J Cell Sci *112 (Pt 6)*, 811-823.

Gauthier, L.R., Charrin, B.C., Borrell-Pages, M., Dompierre, J.P., Rangone, H., Cordelieres, F.P., De Mey, J., MacDonald, M.E., Lessmann, V., Humbert, S., and Saudou, F. (2004). Huntingtin controls neurotrophic support and survival of neurons by enhancing BDNF vesicular transport along microtubules. Cell *118*, 127-138.

Kittler, J.T., Chen, G., Honing, S., Bogdanov, Y., McAinsh, K., Arancibia-Carcamo, I.L., Jovanovic, J.N., Pangalos, M.N., Haucke, V., Yan, Z., and Moss, S.J. (2005). Phospho-dependent binding of the clathrin AP2 adaptor complex to GABAA receptors regulates the efficacy of inhibitory synaptic transmission. Proc Natl Acad Sci U S A *102*, 14871-14876.

Kittler, J.T., Rostaing, P., Schiavo, G., Fritschy, J.M., Olsen, R., Triller, A., and Moss, S.J. (2001). The subcellular distribution of GABARAP and its ability to interact with NSF suggest a role for this protein in the intracellular transport of GABA(A) receptors. Mol Cell Neurosci *18*, 13-25.

Kittler, J.T., Thomas, P., Tretter, V., Bogdanov, Y.D., Haucke, V., Smart, T.G., and Moss, S.J. (2004). Huntingtin-associated protein 1 regulates inhibitory synaptic transmission by

modulating gamma-aminobutyric acid type A receptor membrane trafficking. Proc Natl Acad Sci U S A *101*, 12736-12741.

Li, X.J., Li, S.H., Sharp, A.H., Nucifora, F.C., Jr., Schilling, G., Lanahan, A., Worley, P., Snyder, S.H., and Ross, C.A. (1995). A huntingtin-associated protein enriched in brain with implications for pathology. Nature *378*, 398-402.

Rahman, A., Friedman, D.S., and Goldstein, L.S. (1998). Two kinesin light chain genes in mice. Identification and characterization of the encoded proteins. J Biol Chem *273*, 15395-15403.

Smith, M.J., Pozo, K., Brickley, K., and Stephenson, F.A. (2006). Mapping the GRIF-1 binding domain of the kinesin, KIF5C, substantiates a role for GRIF-1 as an adaptor protein in the anterograde trafficking of cargoes. J Biol Chem *281*, 27216-27228.